Received: 8 December 2022 | Revised: 10 March 2023 | Accepted: 22 March 2023

DOI: 10.1111/jace.19145

Journal of the American Ceramic Society

RESEARCH ARTICLE

Characterization of graphite–chromium carbide composites manufactured by spark plasma sintering

Juan Piñuela-Noval[1] | **Daniel Fernández-González**[1] | **Marta Suárez**[1] | **Luis Antonio Díaz**[1] | **Luis Felipe Verdeja**[2] | **Adolfo Fernández**[1]

[1]Centro de Investigación en Nanomateriales y Nanotecnología (CINN), Consejo Superior de Investigaciones Científicas (CSIC), Universidad de Oviedo (UO), Principado de Asturias (PA), El Entrego, Asturias, Spain

[2]Departamento de Ciencia de Los Materiales e Ingeniería Metalúrgica, Escuela de Minas, Energía y Materiales, Universidad de Oviedo, Calle Independencia, Oviedo, Asturias, Spain

Correspondence
Daniel Fernández-González, Centro de Investigación en Nanomateriales y Nanotecnología (CINN), Consejo Superior de Investigaciones Científicas (CSIC), Universidad de Oviedo (UO), Principado de Asturias (PA), Avda de la Vega 4-6, 33940 El Entrego, Asturias, Spain.
Email: d.fernandez@cinn.es

Funding information
Spanish Ministry of Science and Innovation; Call Programa Estatal de I+D+i Orientada a los Retos de la Sociedad, Grant/Award Number: RTI2018-102269-BI00; Juan de la Cierva-Formación Program, Grant/Award Number: FJC2019-041139; Government of the Principality of Asturias; Call Programa"Severo Ochoa" of Grants for Research and Teaching of the Principality of Asturias, Grant/Award Number: BP20041

Abstract

This manuscript contains an investigation about the influence of the chromium content on the properties of novel graphite–chromium composites obtained by spark plasma sintering (SPS), with great potential application in heat dissipation. Green compacts of 40 mm in diameter were first obtained by uniaxial pressing at 60 MPa, and then the composite was sintered at 1800°C in SPS under vacuum conditions and a pressure of 30 MPa. These sintering conditions involved local liquid phase, which promoted the densification of the composite up to values close to 90%. Different chromium contents were studied, 0, 1, 2, 5, 7, and 10 vol.%, where the best properties (densification, young modulus, electrical conductivity, thermal conductivity, and flexural strength) were obtained in the case of the composite with 7 vol.% Cr: 86.22%, 52.7 GPa, 0.79 MS/m, 264 W/m K, and 38.97 MPa, respectively, measured in the in-plane direction due to the anisotropic behavior of the composite.

KEYWORDS
chromium, composites, electrical conductivity, graphite, mechanical properties, nanomaterials, spark plasma sintering, thermal conductivity

1 | INTRODUCTION

Heat sinks have as objective to transfer thermal energy from a higher-temperature source to a lower-temperature source (generally air). The development of these devices (and the corresponding materials used for their manufacture) has accompanied the progress of equipment, which is more and more small, light, and efficient, particularly not only in the field of electronic devices or mobile phones, but also in other fields where the lightness and performance are more important than the size, as aerospace applications, high-speed trains, and so on. Metals have been traditionally used in applications where high thermal conductivity was required, for instance, copper and alloys (around 400 W/m K) or aluminum (around 250 W/m K). Nevertheless, the problem arises when metallic materials must operate at high temperatures as some of them melt at temperatures <1000°C, although some other difficulties, as creep, appear at temperatures well-below the melting point. Moreover, the requirements of capacity for heat

dissipation are more and more demanding and, sometimes, the thermal conductivity of the metal itself is not sufficient. Therefore, composites metal–metal (copper–tungsten[1]) or metal–diamond (diamond/Cu composites[2]; Cu–0.2% Ti/diamond[3]; Cu–0.3 wt.% B/diamond[4]; Cu–0.5 wt.% Zr/diamond[5,6]) with high thermal conductivity are gaining interest. In some cases, as in Kim et al.,[1] for the Cu–W composites, the value of thermal conductivity is high even at high temperatures (>300 W/m °C at 1000°C, although the best values were measured at around 500°C), which overcomes some of the problems identified in metallic materials, as copper, for instance, which melts at 1085°C. Anyway, those composites with diamond, even when it is one of the highest thermal conductivity materials (2000 W/m K), will be probably difficultly scaled up for wide utilization in thermal management applications due to the price.

Graphite-based composites might be an alternative to the abovementioned materials in thermal management solutions due to the competing advantage of the low density combined with a good thermal conductivity in-plane. In this line, several researchers have investigated high thermal conductivity and low expansion coefficient graphite–copper,[7,8] graphite–aluminum,[9,10] or graphite–magnesium[10] composites with particular interest in the field of electronic industry. Also within the carbon materials, graphene has also attracted interest as additive to improve the thermal conductivity of metals. In this way, Nazeer et al. reported that the addition of 1 wt.% graphene oxide in copper-reduced graphene composites resulted in 80% greater thermal conductivity than in the case of pure copper.[11]

Anyway, graphite matrix composites are the most promising to be used in extreme conditions applications, as rocket nozzles, collimators, or particle accelerators,[12] whether they contain some additive or second phase (molybdenum, copper, diamond, carbon fibers, silicon, silicon carbide, titanium, or tungsten), resulted from the low density and high thermal conductivity. In this line, the addition of reactive metals (particularly niobium, molybdenum, hafnium, tantalum, etc.) to improve the thermal and mechanical properties of the graphite has been studied for at least 50 years,[13,14] although it was not until the last decade when the investigation in this line has received a special attention, particularly in the case of graphite–molybdenum composites due to their potential application as collimators in the CERN (Conseil Européen pour la Recherche Nucléaire) facilities. The interest of graphite–molybdenum composites comes from the excellent mechanical properties conferred by the graphite and molybdenum carbides, which are formed when sintered together, combined with a low density (around 2.5 g/cm^3), refractory character, high thermal stability, and good thermal and electrical conductivities. These graphite–molybdenum composites (and variable amounts of a third phase as titanium, carbon fibers, silicon, silicon carbide or tungsten added to avoid crystallographic transformations, promote the thermal conductivity, increase the resistance to oxidation at high temperatures or improve the mechanical properties) were manufactured by fast novel sintering techniques as rapid hot-pressing of powders mixture[15,16] or spark plasma sintering (SPS),[12,17,18] due to the potential advantages of these techniques regarding high temperatures under a simultaneous application of pressure. Apart from the application in the field of collimators, these graphite–molybdenum composites have been proposed as heat sinks by other authors,[12,18] although their main disadvantage is the sintering temperature, which is above 2000°C. However, other families of graphite–metal composites, that is, graphite–chromium, can solve this problem because this material can provide properties for heat dissipation comparable with those of the graphite–molybdenum–titanium system using sintering temperatures of around 1800°C. Up to now, research within the graphite–chromium system is to be reported, so it is worth studying it. Thus, this manuscript proposes research about the thermal, electrical, and mechanical properties of novel graphite–chromium composites, using SPS technique, for different chromium contents (0, 1, 2, 5, 7, and 10 vol.%).

2 | EXPERIMENTAL PROCEDURES

2.1 | Materials and experimental

Graphite and chromium powders were used as starting materials to prepare graphite–(0, 1, 2, 5, 7, and 10 vol.%) chromium composites.

Graphite (purity of 99%) from Asbury Carbons Company was one of the raw materials used to obtain the samples. The morphology of this crystalline natural graphite was spheroidal flake. The mean particle size, d_{50}, was 6 μm. Spheroidal–flake morphology is useful to promote the compaction of the final composite and, therefore, improve the properties of the sintered composite.[17] Figure 1 provides an image of the graphite powders.

Chromium (purity ≥99%) from Sigma-Aldrich was employed in the experiments. The particles had a spherical–irregular morphology and a mean particle size, d_{50}, of <100 μm. Figure 2 provides an image of the chromium powders used in the composites.

The powder mixtures were prepared in a roller mill (Astursinter S. L. R., Asturias, Spain) using 3 mm alumina balls and a rate of 100 rpm for 24 h to promote the homogenous mixing. Graphite and chromium mixtures (1, 2, 5, 7, and 10 vol.%) were prepared using isopropyl alcohol. This procedure was employed to promote the mixing and ensure a homogeneous material for subsequent steps of

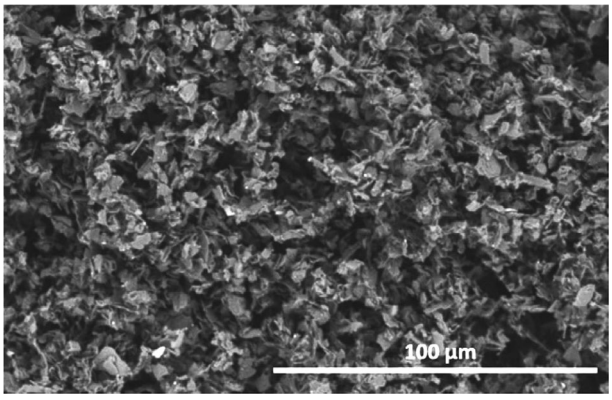

FIGURE 1 Spheroidal–flake morphology graphite used in the experiments.

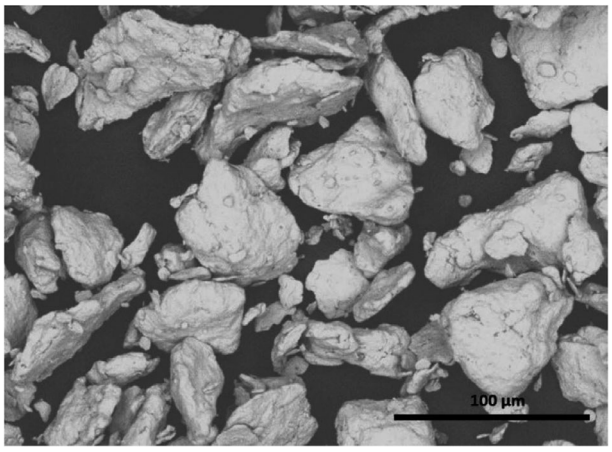

FIGURE 2 Spheroidal–irregular morphology chromium used in the experiments.

the process. Finally, the material was dried at 120°C and sieved through a mesh of 180 μm. Figure 3 corresponds to the powders mixed using the above-reported procedure.

A uniaxial pressure of 60 MPa in metallic mold was used to obtain green compacts that were later placed into a graphite die (40 mm inner diameter) for SPS. The heating cycle up to the sintering temperature had two steps: heating at a rate of 100°C/min from room temperature to 1600°C and heating at 25°C/min from 1600°C to sintering temperature (1800°C). Then, samples were sintered for 20 min of dwell time at 1800°C. A uniaxial pressure of 25 MPa was applied from 1700°C. The temperature was controlled above the sample center using an axial pyrometer focused on the upper graphite punch.

2.2 | Characterization techniques

Field emission scanning electron microscopy on a Quanta FEG 650 was used for the microstructural characterization of the initial raw materials and sintered samples. The

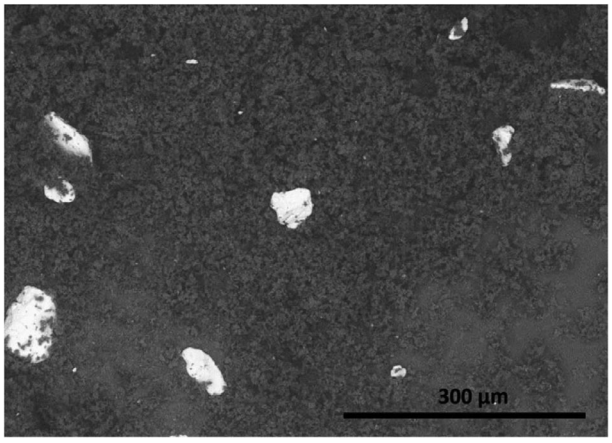

FIGURE 3 Micrograph of the mixed powders, in the image, graphite–10 vol.% chromium.

microstructure of the sintered samples was analyzed on specimens of fracture surface.

Mineralogical phases were identified using X-ray diffraction technique with a Bruker Advanced Powder X-ray diffractometer model D8 with Cu-k_α radiation ($\lambda = 0.15406$ nm). Copper anticathode water cooled with an intensity of 40 mA and a voltage of 40 kV, a swept between 10 and 70° with a step of 0.02° and a step time of 0.2 s were the working conditions. Crystalline phases were determined with the diffraction pattern files of the JCPDS (International Centre for Diffraction Data).

The relative density of the sintered samples was calculated using the following equation:

$$\rho\ (\%) = \frac{d}{d_{th}} \cdot 100 \tag{1}$$

where d is the apparent density determined from measurements of mass and volume (diameter and height) and d_{th} is the theoretical density, determined by helium pycnometer (AccuPyc 1330 V2.04N) on powdered samples (<63 μm) of the sintered composite.

Properties were measured in the in-plane direction of samples, except thermal conductivity. The in-plane direction corresponds to the direction perpendicular to the applied pressure. Thermal parameters were measured in the through-plane direction, and the value in the in-plane direction was indirectly calculated by the modified Wiedemann–Franz law ($\lambda/\sigma = L \cdot T$, where λ is the thermal conductivity, σ is the electrical conductivity, L is the modified Lorenz number, assumed to be the same in the in-plane and through-plane directions, and T is the temperature). The other properties in the through-plane direction cannot be measured because the thickness of the sample (3 mm) obtained in the SPS is not sufficient to machine specimens. Electrical conductivity in the through-plane direction is assumed to be <0.1 MS/m,

which is supported by the experimental results[12,17,18] for other highly oriented graphite–metal composites, and it is very conservative because the values in this direction are usually 20%–40% lower.[16,17] Values in the through-plane direction are usually between 0.05 and 0.08 MS/m.[17] Wiedemann–Franz law can be applied with sufficient accurateness in graphite–metal composites although with a modified number of Lorenz. In fact, the Wiedemann–Franz law has been applied in other materials different to the metals as carbides,[19,20] polymers,[21] and even graphite.[22,23] The application of the Wiedemann–Franz law in graphite–molybdenum composites provides values of the modified Lorenz number for the in-plane and through-plane directions that do not differ in more than 10% (habitually around 4%–5%).

Samples of 3 mm × 4 mm × 20 mm were prepared to measure the bending strength using the Shimadzu-Series AGS-IX tests machine. Bending strength (σ_f, in MPa) of material after the three-point bending test was evaluated using the following equation:

$$\sigma_f = \frac{3 \cdot P \cdot L}{2 \cdot w \cdot b^2} \quad (2)$$

where P is the failure load in N, L is the distance between supports (span, 12.5 mm) in mm, w is the width of the sample in mm, and b is the thickness of the sample in mm.

Four-point probe measurement technique in the in-plane direction using the equipment PSM1735—NumetriQ—Newtons fourth was employed to determine the electrical conductivity.

Young's modulus was determined on sintered samples of 3 mm × 4 mm × 20 mm (in-plane) with the equipment GrindoSonic (MK, Belgium).

Thermal conductivity was indirectly calculated from the thermal diffusivity (α, mm^2/s), the specific heat (c_p, J/g K), and the density (d, g/cm^3) using the following equation:

$$\lambda = \alpha \cdot d \cdot c_p \quad (3)$$

where λ is the thermal conductivity (W/m K). The measurement of the thermal diffusivity was carried out in the equipment LFA 457 MicroFlash from Netzsch at 25°C on specimens of 10 mm × 10 mm × 3 mm. Specific heat was determined using a C80 (Setaram Instrumentation) calorimeter, equipped with stainless steel cells (S60/1413), in continuous mode, using a heating ramp of 0.1°C/min from 20 to 40°C, with 2 h of stabilization at the start and end temperatures. The data processing was carried out using the Calisto Software.

Coefficient of thermal expansion (CTE) of the graphite–chromium composite was measured in the temperature range from 30 to 150°C in dilatometer equipment (Netzsch DIL402C, Germany). The sample was measured in the in-plane direction (specimen of 5 mm in length, 3 mm in thickness, and 4 mm in width) and in the through-plane direction (specimen of 3 mm in length, 5 mm in thickness, and 4 mm in width).

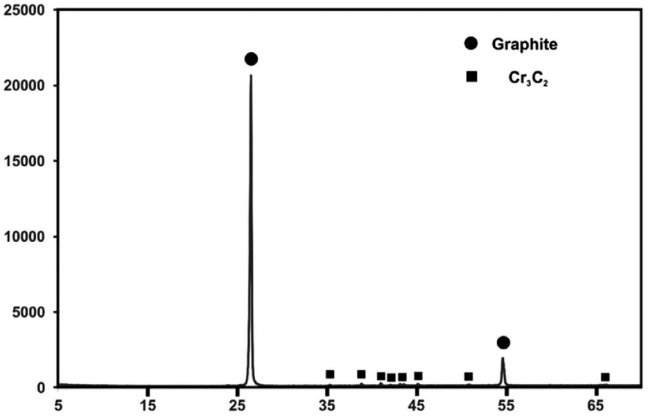

FIGURE 4 X-ray diffraction pattern of the sample graphite–7 vol.% Cr previously uniaxially pressed at 60 MPa and then spark plasma sintering (SPS) sintered at 1800°C–20 min. X-ray diffraction patterns are analogous for the other compositions with changes only in the intensity of the peaks.

3 | RESULTS

3.1 | Phase composition

Figure 4 corresponds to the X-ray diffraction analysis of the sintered specimen, where graphite and chromium (II) carbide are identified.

3.2 | Microstructure

Figure 5a,b corresponds to a sample graphite–7 vol.% Cr, where the chromium (II) carbide appears homogeneously distributed within the matrix of graphite. The disposition of graphite lamellae in the perpendicular direction to the pressure can be seen in Figure 5a. Moreover, it is also possible to identify that chromium (II) carbide appears filling empty spaces in the composite (Figure 5b).

3.3 | Properties

3.3.1 | Density

Relative density of the sintered powders was calculated using Equation (1) and the values are collected in Table 1. Relative density grows as the chromium content in the

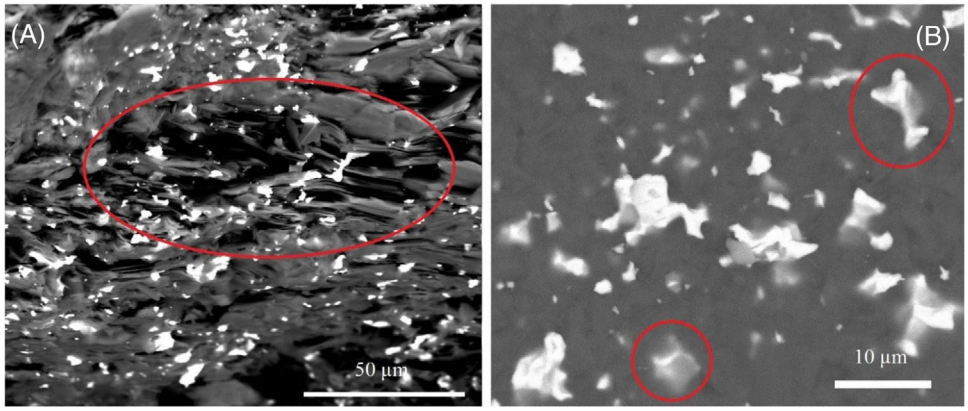

FIGURE 5 Scanning electron microscopy (SEM) images of the sample graphite–7 vol.% Cr previously uniaxially pressed at 60 MPa and then spark plasma sintering (SPS) sintered at 1800°C–20 min: (a) graphite lamellae oriented perpendicular to the pressing visible on fracture surface; (b) chromium carbides appear filling the spaces between grains.

TABLE 1 Density values of the green compacts, apparent density, real and relative density.

Sample	Theoretical density, d_{th} (g/cm^3)s	Apparent density, d (g/cm^3)	Relative density (%)
Graphite	2.2661	1.7337	76.51
Graphite–1 vol.% Cr	2.3101	1.8675	80.84
Graphite–2 vol.% Cr	2.3567	1.9247	81.67
Graphite–5 vol.% Cr	2.5205	2.0987	83.26
Graphite–7 vol.% Cr	2.6422	2.2932	86.79
Graphite–10 vol.% Cr	2.7381	2.3533	85.95

TABLE 2 Electrical conductivity values of the spark plasma sintering (SPS)-samples.

Sample	Electric conductivity (MS/m) (in-plane)
Graphite	0.04 ± 0.01
Graphite–1 vol.% Cr	0.06 ± 0.01
Graphite–2 vol.% Cr	0.12 ± 0.01
Graphite–5 vol.% Cr	0.20 ± 0.02
Graphite–7 vol.% Cr	0.79 ± 0.14
Graphite–10 vol.% Cr	0.45 ± 0.10

composite increases, except for the greatest chromium content (10 vol.% Cr).

3.3.2 | Electrical conductivity

Electrical conductivity values are collected in Table 2. Values of electrical conductivity increase as the chromium content increases except for the sample graphite–10 vol.% Cr.

TABLE 3 Values of the thermal conductivity in the through-plane direction.

Sample	Thermal conductivity (W/m K) (through-plane)	Thermal conductivity (W/m K) (in-plane)
Graphite	13.78	5.25
Graphite–1 vol.% Cr	15.72	9.56
Graphite–2 vol.% Cr	18.44	22.05
Graphite–5 vol.% Cr	29.02	58.94
Graphite–7 vol.% Cr	33.63	264.13
Graphite–10 vol.% Cr	26.06	131.90

3.3.3 | Thermal conductivity

Thermal conductivity values are collected in Table 3, both for the through-plane and in-plane directions. Values in the in-plane direction are significantly greater than in the through-plane direction for chromium contents above 5 vol.%. The values of thermal conductivity in-plane and through-plane directions for chromium content below 5 vol.% are on the same order of magnitude due to the poor densification. The differences in the values in Table 3 are consequence of the assumptions and mathematical calculations indicated in Section 2.2.

3.3.4 | Young's modulus

Young's modulus values are collected in Table 4, where the behavior of the value is similar to that observed in the case of other properties.

TABLE 4 Values of the young modulus of the spark plasma sintering (SPS)-samples.

Sample	Young modulus (GPa)
Graphite	22.53 ± 0.10
Graphite–1 vol.% Cr	23.34 ± 0.12
Graphite–2 vol.% Cr	27.09 ± 0.52
Graphite–5 vol.% Cr	45.50 ± 0.29
Graphite–7 vol.% Cr	52.73 ± 0.46
Graphite–10 vol.% Cr	46.39 ± 0.57

TABLE 5 Values of the bending strength.

Sample	Bending strength (MPa)
Graphite	23.93 ± 3.63
Graphite–1 vol.% Cr	18.95 ± 1.26
Graphite–2 vol.% Cr	21.36 ± 1.51
Graphite–5 vol.% Cr	30.87 ± 2.17
Graphite–7 vol.% Cr	38.97 ± 2.27
Graphite–10 vol.% Cr	42.71 ± 0.72

3.3.5 | Bending strength

Values of the bending strength appear in Table 5. The best results were obtained, as opposed to other cases, for the graphite–10 vol.% Cr (42.71 MPa), although without significant differences with the composite graphite–7 vol.% Cr (38.97 MPa).

4 | DISCUSSION

Graphite–metal composites have found interest in different fields, particularly for extreme conditions applications, as collimators for CERN.[15,16,17] However, these graphite–metal composites might be used in heat dissipation. The great advantage of graphite–metal composites is the refractory character, the high thermal stability, the physical and mechanical properties as well as the thermal and electrical conductivities. Despite the potential interest of graphite–metal composites in the above-reported applications, researchers focused only on the graphite–molybdenum system. Nevertheless, there are other graphite–metal systems with promising possibilities in this line. This is the case of the graphite–chromium system, which has never been reported in the literature. Sintering in the graphite–chromium system, as opposed to the graphite–molybdenum, requires from lower temperatures. Sintering temperatures of 1800°C are sufficient to consolidate the starting powders in presence of liquid, which is at least 200°C lower than that required for the sintering of graphite–molybdenum composites.[12,17] Time is also shorter, as the sintering cycle (heating + dwell time + cooling in SPS) takes 44 min + cooling in SPS equipment in front of the 131 min + cooling in the SPS apparatus required in the graphite–molybdenum system.[12] The competitive advantage of the C–Cr system, in comparison with the C–Mo system, is precisely the temperature required for the liquid phase sintering. In the C–Cr binary diagram, there is a phase transformation at a temperature of 1811°C, whereas in the C–Mo binary diagram, the phase transformation that involves liquid phase takes place at 2584°C, for the compositions studied in this system. These temperatures required for the appearance of liquid phase are slightly lower in the SPS due to both the vacuum conditions and the pressure applied in the process. Therefore, sintering in this research occurred in presence of liquid phase as it is clearly visible in Figure 5b, where liquid chromium appears in triple points and grain boundaries. In fact, it is not chromium but chromium (II) carbide, as it was identified in the X-ray diffraction analysis in Figure 4. This is consistent with the carbon–chromium diagram, which for the compositions studied in this manuscript, indicates that graphite and Cr_3C_2 are the stable phases at room temperature. The Cr_3C_2 is formed by reaction of the solid (graphite) and liquid (chromium), where carbon atoms dissolve in the liquid phase and diffuse, and eventually carbon structures are built to sinter together the graphite powders into solid graphite. The solidification of the liquid phase results into Cr_7C_3 + Cr_3C_2, but with excess carbon composition and unimpeded carbon diffusion, the system moves to the Cr_3C_2 + C zone.[24] The presence of the liquid phase promotes the densification of the composite, with a maximum of relative density for the composite with 7 vol.% Cr (Table 1). This can be explained because there is an excess of liquid phase for greater chromium contents (10 vol.%), for the conditions of pressure and temperature in the SPS, that migrates in minor quantities to the borders of the sample and appears deposited in the walls of the mold after the sintering process. This leads to a reduction in the densification (and material losses), which is translated later into the thermal, electrical, and mechanical properties of the composite. Values of relative density do not significantly exceed the 85%, which is consistent with the information provided by Aguiar et al.[25] that indicates that densification above 85% is difficulty reached in the case of graphite materials. Within the graphite–metal composites, it is necessary to apply relatively high pressures to obtain the green compacts. Guardia-Valenzuela et al.,[17] for the graphite–molybdenum–titanium system employed a pressure of 300 MPa to obtain the green compacts, although Suárez et al.[18] observed that using pressures >60 MPa did not translate into a significant increase in the value of the

density of the green compacts. Therefore, considering the similitude between the graphite–Mo and graphite–Cr systems, a pressure of 60 MPa was applied, and it was seen sufficient to see an alignment of the graphite in the direction perpendicular to the pressing, as it is observed in Figure 5a. Later, the applied pressure in the SPS machine produces a further alignment of the graphite flakes in the basal direction, which ensures a directional behavior with the best properties being measured in the in-plane direction. In this way, liquid chromium–chromium carbides migrate throughout the lamellae of graphite preferentially in the in-plane direction, filling spaces as in Figure 5b, which enhances further the anisotropic behavior of these composites.

The anisotropic behavior of graphite regarding electrical conductivity was already reported in the forties of the last century.[26] For instance, thermal pyrolytic graphite in the in-plane direction exhibits an electrical conductivity of 2.4 MS/m. Other research studies for graphite with metal additions (molybdenum, titanium) have reported values of the electrical conductivity approaching 1 MS/m in the in-plane direction: 0.88–1.01 MS/m in-plane by Guardia-Valenzuela et al.[17]; 0.86 MS/m in-plane by Suárez et al.[18]; or, 0.99 MS/m in-plane by Suárez et al.[12] The greatest value reported in this manuscript measured in the in-plane direction is 0.79 MS/m, which is not far from these values. The influence of the chromium carbide in the promotion of the electrical conductivity is clearly observed in Table 2, which is also consistent with the trend of the relative density indicated in Table 1 and the problems of chromium losses by extrusion identified in the sample with 10 vol.% Cr. The high electrical conductivity in the sample with 7 vol.% Cr can be explained by the initial graphite flakes bonded together in a highly oriented matrix with chromium carbides being the main responsible of the high electrical conductivity. This behavior is translated into the thermal conductivity due to the parallelism between the electrical and thermal behaviors. In this line, the electrical conductivity of the chromium (II) carbide is 13.33 MS/m[27] while that of the graphite in the basal plane approaches 1 MS/m,[28] although it is possible to see that the value of the electrical conductivity of the graphite sintered in the SPS apparatus is well-below this value (0.04 MS/m) whether second phases are not added. Therefore, it is the chromium carbide the responsible of the electrical (and thermal) conductivity of the composite. Densification also plays an important role in the electrical (thermal and mechanical properties), as electrical conductivity is directly related to the densification of the composite, according to the results in Tables 1 and 2. Thus, in this line, it is possible to find works of researchers who studied what would be the critical volume that leads the graphite–air being insulating[29] and determined how the orientation of the graphite is important for the electrical conductivity of graphite-based composites.[30] Phenomena that explain the difficulty of reaching high values of electrical conductivity without employing metallic or metal carbide additives. So, liquid chromium (II) carbide can more easily displace in the in-plane direction due to both the orientation of the graphite planes produced by the pressure applied to obtain the green compacts and the pressure during the sintering process in the SPS. This, apart from the promotion of the densification of the composite, provides more metallic continuity in the in-plane direction, which apart from the influence on the thermal and electrical properties of the composite reflects into the mechanical properties of the composite. Reducing the chromium content decreases the importance of this mechanism. The values of thermal conductivity are comparable with those proposed by Guardia-Valenzuela et al.[17] (in-plane, 647−740 W/m K; through-plane, 56−50 W/m K), Suárez et al.[12] (in-plane, 136.68 W/m K; through-plane, through-plane, 22.09 W/m K), and Suárez et al.[18] (in-plane, 201.49 W/m K; through-plane, 23.43 W/m K) for graphite–molybdenum–titanium composites, which indicates that the graphite–chromium composites could be used in the field of heat sinks with similar behavior regarding thermal conductivity but with lower sintering temperature. Graphite itself, even when it can reach very high thermal conductivity values in highly oriented thermal pyrolytic graphite (up to 1900 W/m K[31]), does not exhibit such values of thermal conductivity in this case. Thermal conductivity is very far from these values in the graphite sintered with the SPS apparatus, which suggests that the increase of the thermal conductivity is directly related to not only the improvement of the densification produced when the chromium content increases but also by the own chromium, which has a thermal conductivity of around 190 W/m K.[32]

Regarding the mechanical properties of the composite, these follow a trend like that of the thermal and electrical properties. Values of the young's modulus are in clear correlation with the relative density values collected in Table 1, and also with chromium content in the sample. It is important to consider that chromium (II) carbide has a young's modulus of around 373 GPa according to Powell and Schofield,[22] whereas that of graphite sintered using the SPS apparatus is 22.53 GPa (for a relative density of 76%). Therefore, chromium carbide is responsible for the increasing value of the young modulus, although the densification has a relevant role that explains the deterioration of the young modulus for the composite with 10 vol.% Cr (together with the potential chromium (II) carbide losses produced by extrusion during the sintering process). The increase of the resistance as the chromium content increases is the result of chromium (II) carbide

that improves the mechanical resistance of the composite. The mechanical resistance, as in the case of the graphite–molybdenum composites, is thought to be conferred by the strong carbide–graphite bond, which provides bridges not only in the in-plane direction but also in the perpendicular direction and limits the basal plane slip (shear) and the delamination.

Results suggest that the best composite is that formed by graphite and 7 vol.% Cr, which provides the greatest values of electrical and thermal conductivities with a bending strength comparable with that of the composite with 10 vol.% Cr, which is the composite with the greatest value in this parameter. The CTE is important for the materials that are going to be used in heat dissipation because they should be cooperative with the rest of the structure of the device. The CTE was determined for this sample graphite–7 vol.% Cr in the in-plane direction and in the through-plane direction. The values are $3.21{\cdot}10^{-6}$ and $12.82{\cdot}10^{-6}$ K^{-1}, respectively. Apart from the low values, whether compared with those of other conventional materials used in heat dissipation as the aluminum ($25.5{\cdot}10^{-6}$ K^{-1}) or copper ($16.7{\cdot}10^{-6}$ K^{-1}), they are comparable with other competing composite alternatives including diamond, that is, Al-diamond or Cu-diamond, although the advantage of the graphite–chromium composite is the lower weight. The coefficients of thermal expansion allow defining an isotropy ratio, by relation between the property in the in-plane direction and the value in the through-plane direction, which is:

$$\mathrm{IR} = \frac{\mathrm{CTE}_{\perp}}{\mathrm{CTE}_{||}} = \frac{3.21 \cdot 10^{-6}\ \mathrm{K}^{-1}}{12.82 \cdot 10^{-6}\ \mathrm{K}^{-1}} = 0.2504 \qquad (4)$$

where $\mathrm{CTE}_{\perp}$ is the CTE in the in-plane direction (perpendicular direction to the applied pressure), whereas $\mathrm{CTE}_{||}$ is the CTE in the through-plane direction (parallel direction to the applied pressure). A value equal or close to 1 indicates an isotropic material,[33] whereas the smaller the IR, the more anisotropic the composite is. Considering the criteria of Seehra et al.,[34] this composite with a ratio $\mathrm{CTE}_{\perp}/\mathrm{CTE}_{||}$ closer to zero is very anisotropic.

The anisotropic behavior of the composite was studied in detail with the support of the X-ray diffraction technique. X-ray spectra were obtained in the in-plane and through-plane directions using 2θ continuous scanning method at a scanning rate of 1°/min, within the range 10°–60° as in Lee et al.[35] A parameter called Da was obtained by using the values of the intensity of the peaks corresponding to the planes (0 0 2) and (1 0 0) as follows:

$$Da = \frac{I_{100}}{I_{100} + I_{002}} \qquad (5)$$

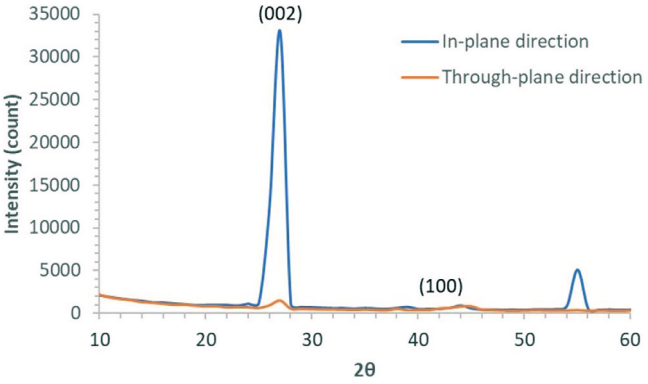

FIGURE 6 X-ray diffractometer spectra of the sintered specimen graphite–7 vol.% Cr in the in-plane (blue) and through-plane (orange) directions.

The X-ray spectra in the in-plane and through-plane directions are collected in Figure 6. The peaks corresponding to the planes (0 0 2) and (1 0 0) appear in the angles 27° (32 942 counts in the in-plane direction and 1469 counts in the through-plane direction) and 42° (548 counts in the in-plane direction and 562 counts in the through-plane direction).

Using Equation (5), the values of the $\mathrm{Da}_{\perp}$, corresponding to the in-plane X-ray diffractogram, and $Da_{||}$, corresponding to the through-plane diffractogram, are 0.2767 and 0.0164, respectively. The anisotropy ratio is calculated as the relation between the $\mathrm{Da}_{\perp}$ and $Da_{||}$ as $\mathrm{Da}_{\perp}/\mathrm{Da}_{||}$. The value is 16.87, which indicates the clear anisotropic behavior of graphite–chromium composites, because the greater the value the more anisotropic the material is.

5 | CONCLUSIONS

A family of graphite-matrix composite material containing chromium particles (chromium carbide, Cr_3C_2, after sintering) has been successfully developed for heat management applications. Composites are produced by SPS assisted by molten metal–carbon liquid phase. Different chromium contents were studied (0, 1, 2, 5, 7, and 10 vol.%) to evaluate the influence of this element in the thermal, electrical, and mechanical properties of the composite (densification, young's modulus, electric conductivity, thermal conductivity, and flexural strength).

As the composite mainly consists of oriented graphite, the material exhibits anisotropic properties with in-plane properties comparable to those of the already investigated graphite–molybdenum composites. In fact, the anisotropy of the composite was studied using CTE and X-ray diffraction technique, which confirm this behavior. As the sintering temperature (1800°C) is well-bellow that required

for the graphite–molybdenum composites (up to 2600°C), the production of graphite–chromium composites might be a competing alternative that could be easier scaled up to industrial level and being a competitor for thermal management applications.

The best values of thermal, electrical, and mechanical properties were obtained in the case of graphite–7 vol.% Cr (densification, young modulus, electric conductivity, thermal conductivity, and flexural strength): 86.22%, 52.7 GPa, 0.79 MS/m, 264 W/m K, and 38.97 MPa, respectively. Greater chromium content resulted in liquid metal losses during the sintering process, which is detrimental for the properties of the composite, particularly for the thermal and electrical conductivities, whose values are a 40% lower.

ACKNOWLEDGMENTS

This research was funded by the Spanish Ministry of Science and Innovation, Call Programa Estatal de I+D+i Orientada a los Retos de la Sociedad (RTI2018-102269-B-I00). Daniel Fernández-González acknowledges the grant (Juan de la Cierva-Formación Program) FJC2019-041139-I funded by MCIN/AEI/10.13039/501100011033 (Ministerio de Ciencia e Innovación, Agencia Estatal de Investigación). Juan Piñuela Noval acknowledges the Programa "Severo Ochoa" of Grants for Research and Teaching of the Principality of Asturias for the funds received for the elaboration of the Ph. D. Thesis (Ref: BP20 041). Authors are grateful to Ainhoa Macías San Miguel from Nanomaterials and Nanotechnology Research Center (CINN) for providing technical assistance.

REFERENCES

1. Kim YDo, Oh NL, Oh S-T, Moon In-H. Thermal conductivity of W–Cu composites at various temperatures. Mater Lett. 2001;51:420–4.
2. Shen X-Y, He X-B, Ren S-B, Zhang H-M, Qu X-H. Effect of molybdenum as interfacial element on the thermal conductivity of diamond/Cu composites. J Alloys Compd. 2012;529:134–9.
3. Yang L, Sun L, Bai W, Li L. Thermal conductivity of Cu-Ti/diamond composites via spark plasma sintering. Diamond Relat Mater. 2019;94:37–42.
4. Bai G, Li N, Wang X, Wang J, Kim MJ, Zhang H. High thermal conductivity of Cu-B/diamond composites prepared by gas pressure infiltration. J Alloys Compd. 2018;735:1648–53.
5. Li J, Wang X, Qiao Yi, Zhang Y, He Z, Zhang H. High thermal conductivity through interfacial layer optimization in diamond particles dispersed Zr-alloyed Cu matrix composites. Scr Mater. 2015;109:72–5.
6. Wang L, Li J, Bai G, Li N, Wang X, Zhang H, Wang J, Kim MJ. Interfacial structure evolution and thermal conductivity of Cu-Zr/diamond composites prepared by gas pressure infiltration. J Alloys Compd. 2019;781:800–9.
7. Yang W, Zhou L, Peng K, Zhu J, Wan L. Effect of tungsten addition on thermal conductivity of graphite/copper composites. Composites B: Eng. 2013;55:1–4.
8. Byun M, Kim D, Sung K, Jung J, Song Y-S, Park S, Son I. Characterization of copper–graphite composites fabricated via electrochemical deposition and spark plasma sintering. Appl Sci (Basel). 2019;9:2853.
9. Chen JK, Huang IS. Thermal properties of aluminum–graphite composites by powder metallurgy. Composites B: Eng. 2013;44:698–703.
10. Oddone V, Boerner B, Reich S. Composites of aluminum alloy and magnesium alloy with graphite showing low thermal expansion and high specific thermal conductivity. Sci Technol Adv Mater. 2017;18:180–6.
11. Nazeer F, Ma Z, Gao L, Wang F, Khan MA, Malik A. Thermal and mechanical properties of copper-graphite and copper-reduced graphene oxide composites. Composites B: Eng. 2019;163:77–85.
12. Suárez M, Fernández-González D, Díaz LA, Borrell A, Moya JS, Fernández A. Synthesis and processing of improved graphite-molybdenum-titanium composites by colloidal route and spark plasma sintering. Ceram Int. 2021;47:30993–8.
13. White JL, Pontelandolfo JM. Graphite-carbide materials prepared by hot-working with a dispersed liquid-carbide phase. Carbon. 1966;4:305–14.
14. Harada Y, Rubin GA. Fabrication and characterization of metal carbide-graphite composites. In: Paper presented at the 68th Annual Meeting of the American Ceramic Society. 1966 May 9. Washington, D C, USA. (https://ntrs.nasa.gov/api/citations/19680009751/downloads/19680009751.pdf)
15. Bertarelli A, Bizarro S. A molybdenum carbide/carbon composite and manufacturing method. World Patent PCT/EP2013/072818. Oct. 2013.
16. Mariani N. Development of novel. In: Advanced molybdenum-based composites for high energy physics applications. Ph.D. Thesis. Milan (Italy): Milan Polytechnic; 2014.
17. Guardia-Valenzuela J, Bertarelli A, Carra F, Mariani N, Bizzaro S, Arenal R. Development and properties of high thermal conductivity molybdenum carbide – graphite composites. Carbon. 2018;135:72–84.
18. Suárez M, Fernández-González D, Gutiérrez-González CF, Díaz LA, Borrell A, Moya JS, et al. Effect of green body density on the properties of graphite-molybdenum-titanium composite sintered by spark plasma sintering. J Eur Ceram Soc. 2022;42:2048–54.
19. Schultrich B, Poeβnecker W. Thermal conductivity of cemented carbides. J Therm Anal. 1988;33(1):305–10. https://doi.org/10.1007/bf01914616
20. Jiang Q, Zeng X, Hu C. A promising layered thermoelectric metallic ceramic with ultra-high temperature stability: Mo2Ti2AlC3, J Alloys Compd. 2022;922:166212. https://doi.org/10.1016/j.jallcom.2022.166212
21. Upadhyaya M, Boyle CJ, Venkataraman D, Aksamija Z. Effects of disorder on thermoelectric properties of semiconducting polymers. Sci Rep, 2019;9:5820. https://doi.org/10.1038/s41598-019-42265-z
22. Powell RW, Schofield FH. The thermal and electrical conductivities of carbon and graphite to high temperatures. Proc Phys Soc. 1939;51(1):153–72. https://doi.org/10.1088/0959-5309/51/1/317
23. Cermak M, Perez N, Collins M, Bahrami M. Material properties and structure of natural graphite sheet. Sci Rep. 2020;10:18672. https://doi.org/10.1038/s41598-020-75393-y

24. Guardia-Valenzuela J. Optimisation of graphite matrix composites for collimators in the LHC upgrade. Ph.D. Thesis. Zaragoza (Spain): University of Zaragoza; 2019.
25. Aguiar JA, Kwon S, Coryell BD, Eyerman E, Bokov AA, Castro RHR, et al. Densification of graphite under high pressure and moderate temperature. Mater Today. 2020;22:100821.
26. Krishnan KS, Ganguli N. Large anisotropy of the electrical conductivity of graphite. Nature. 1939;144:667.
27. Tulhoff H. Carbides. In: ULLMANN'S encyclopedia of industrial chemistry. Weinheim: Wiley-VCH Verlag GmbH & Co; 2012. p. 565–82.
28. Yemata TA, Ye Q, Zhou H, Kyaw AKK, Chin WS, Xu J et al. 6 – Conducting polymer-based thermoelectric composites: principles, processing, and applications. In: Thakur VK, Thakur MK, Pappu A, editors. Hybrid polymer composite materials. Kidlington: Woodhead Publishing; 2017. p. 169–95.
29. Deprez N, Mclachlan DS. The analysis of the electrical conductivity of graphite conductivity of graphite powders during compaction. J Phys D: Appl Phys. 1988;21:101.
30. Marinković S, Sužnjević C, Djordjević M. Pressure dependence of the electrical resistivity of graphite powder and its mixtures. Phys Status Solidi A: App Mater Sci. 1971;4:743–54.
31. Klemens PG, Pedraza DF. Thermal conductivity of graphite in the basal plane. Carbon. 1994;32:735–41.
32. Shackelford JF, Han Y-H, Kim S, Kwon S-H et al. CRC Materials science and engineering handbook. London: CRC Press; 2015.
33. Lee S-M, Kang D-Su, Roh J-S. Bulk graphite: materials and manufacturing process. Carbon Lett. 2015;16:135–46.
34. Seehra MS, Pavlovic AS, Babu VS, Zondlo JW, Stansberry PG, Stiller AH. Measurements and control of anisotropy in ten coal-based graphites. Carbon. 1994;32:431–5.
35. Lee S-M, Kang D-Su, Kim W-S, Roh J-S. Fabrication of isotropic bulk graphite using artificial graphite scrap. Carbon Lett. 2014;15:142–15.

How to cite this article: Piñuela-Noval J, Fernández-González D, Suárez M, Díaz LA, Verdeja LF, Fernández A. Characterization of graphite–chromium carbide composites manufactured by spark plasma sintering. J Am Ceram Soc. 2023;106:5157–5166. https://doi.org/10.1111/jace.19145